THE JOURNAL OF PHYSICAL CHEMISTRY A LETTERS

2007, *111,* 411−414
Published on Web 12/30/2006

Dual Relationship between Large Gold Clusters (Antifullerenes) and Carbon Fullerenes: A New Lowest-Energy Cage Structure for Au_{50}

Dongxu Tian,[†] Jijun Zhao,*[,‡] Baolin Wang,[§] and R. Bruce King[||]

Department of Chemistry, Dalian University of Technology, Dalian 116024, China, State Key Laboratory of Materials Modification by Laser, Electron, and Ion Beams & College of Advanced Science and Technology, Dalian University of Technology, Dalian 116024, China, Department of Physics, Huaiyin Institute of Technology, Jiangsu 223001, China, and Department of Chemistry and Center for Computational Chemistry, University of Georgia, Athens, Georgia 30602

Received: September 25, 2006; In Final Form: November 14, 2006

Recent theoretical prediction and experimental confirmation of cage configurations for Au clusters have stimulated considerable interest in finding novel gold clusters exhibiting high stability. We use a dual relationship between gold antifullerene cages with all triangular faces and carbon fullerenes with all degree 3 vertices to construct a large number of Au_{50} antifullerene cages by omnicapping and dualization procedures. Among these cages we find a new D_{6d} cage as the lowest-energy configuration of Au_{50}. The unusual stability of this new Au_{50} cage is associated with spherical aromaticity and sp-d hybridization.

Low-dimensional gold nanostructures have been the focus of intensive studies owing to their importance in catalysis and nanoelectronics.[1−6] In addition, the relativistic effect of interatomic Au−Au bonding leads to unusual atomic structures.[4] Thus, neutral and charged Au_n clusters are generally believed to be planar,[7−10] which is supported by experimental photoelectron spectra,[11−13] although there have been some controversies about the critical size for the planar-to-nonplanar transition. Furthermore, an unexpected macrotetrahedral configuration of Au_{20} with T_d symmetry, which is indeed a piece of bulk face-centered cubic (fcc) lattice with four (111) faces, is indicated by photoelectron spectroscopy combined with first-principles density functional theory (DFT) calculations.[14] For still larger Au_n clusters with $n > 20$, hollow cage configurations are predicted to prevail over conventional compact structures[15−17] at Au_{32}[18,19] as well as Au_{50}[20] from DFT calculations. The unusual stability of these all-metal hollow cages has been attributed to spherical aromaticity and relativistic effects.[18−20] An icosahedral cage (so-called "golden fullerene" but really an "antifullerene") has also been proposed as a local minimum for Au_{42},[21] which is competitive energetically with the compact configurations. However, unlike the Au_{32} and Au_{50} cages, Au_{42} does not satisfy the $2(k + 1)^2$ rule of spherical aromaticity.[22] Other than fullerene-cased cages, a highly symmetric tube-like cage was predicted to be a possible ground-state structure for Au_{26}.[23] Very recently, free-standing hollow cages were identified for anionic Au_{16}^-, Au_{17}^-, and Au_{18}^- clusters by a combined photoelectron spectroscopy/DFT study.[24] In the case of one-dimensional nanostructures, ultrathin gold nanotubes have been synthesized and observed by transmission electron microscope.[25]

Since the discovery of carbon fullerenes with free-standing hollow cages,[26] increasing interest has arisen in finding novel clusters or molecules of other elements exhibiting similar cage configurations.[27−30] Such efforts have been stimulated by the discovery of planar, cage, and tubular structures in aggregates of gold atoms. However, the chemical bonding is very different in carbon and gold structures. In a carbon structure, including the fullerenes as well as planar graphite, an sp^2 carbon atom forms three bonds with other atoms on the planar graphene sheet or curved fullerene surface. However, in planar gold clusters or nanotubes, the gold atoms typically form five or six Au−Au bonds with other gold atoms in networks typically constructed by fusing Au_3 triangles. This leads to a dual relationship between the graphene sheet surface and a single-layer slab of Au (111) surface where the centers of the hexagons in the graphene sheet correspond to gold atom vertices in the Au(111) surface. Furthermore, the centers of the Au_3 triangles in the Au(111) surface correspond to carbon atom vertices in the graphene sheet. Because of this dual relationship between the carbon fullerenes with all degree 3 carbon vertices and the gold clusters with all triangular faces, the gold clusters are conveniently called antifullerenes.

This dual relationship leads to two procedures for constructing gold cluster structures from graphene sheets or fullerene polyhedra. Thus, adding one atom in the center of each hexagon ring in the graphene sheet followed by rescaling by a factor of 2.031, relating to the bond distance ratio r(Au−Au)/r(C−C), leads to a single-layered Au (111) slab. This procedure is called omnicapping. Alternatively, if the addition of an atom in the center of each hexagon ring in the graphene sheet is followed by removal of all of the vertex atoms in the original hexagon

* To whom correspondence should be addressed. E-mail: zhaojj@dlut.edu.cn.
[†] Department of Chemistry, Dalian University of Technology.
[‡] State Key Laboratory of Materials Modification by Laser, Electron, and Ion Beams & College of Advanced Science and Technology, Dalian University of Technology.
[§] Huaiyin Institute of Technology.
[||] University of Georgia.

10.1021/jp066272r CCC: $37.00

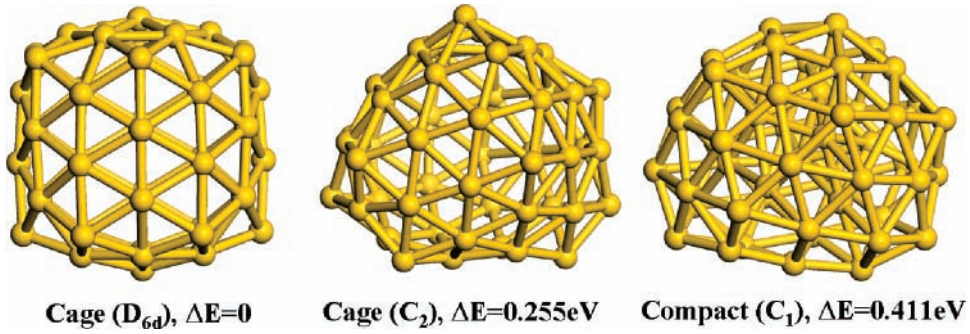

Figure 1. Lowest-energy cage and compact configurations of Au_{50} antifullerene from present DFT calculations and previous work.[20] The energy difference between C_2 and C_1 isomers is 0.156 eV, comparable to previous result of 0.178 eV.

rings, the same Au (111) slab is obtained after a simple rescaling by a factor of 1.172. This latter procedure is called *dualization* and leads to familiar pairs of dual polyhedra. Thus, a given polyhedron $\mathscr{P}$ can be converted into its dual $\mathscr{P}^*$ by locating the centers of the faces of $\mathscr{P}^*$ at the vertices of $\mathscr{P}$ and the vertices of $\mathscr{P}^*$ above the centers of the faces of $\mathscr{P}$. Two vertices in the dual $\mathscr{P}^*$ are connected by an edge when the corresponding faces in $\mathscr{P}$ share an edge. For example dualization of a cube leads to an octahedron.

The capping and dualization procedures establish connections between carbon fullerenes and gold antifullerenes. For instance, the Au_{32} cage with I_h symmetry[18,19] can be obtained either by omnicapping a C_{20} fullerene or by dualization of a C_{60} fullerene. Similarly the Au_{42} cage[22] can be obtained by dualization of the C_{80} fullerene isomer with I_h symmetry. Furthermore, the Au_{50} cage reported in ref 20 arises from omnicapping a C_{32} fullerene. We have now studied gold antifullerenes with 50 Au atoms constructed by dualization of fullerene C_{96} isomers. This C_{96} fullerene dualization process has led to a number of Au_{50} antifullerene cages having lower total energies than the previously reported Au_{50} cage[20] obtained by omnicapping a C_{32} fullerene. Moreover, the lowest-energy Au_{50} antifullerenes found in this work can be viewed as embryos of a single-walled gold nanotube.

The initial structures of the fullerene cages were taken from the fullerene structure library.[31] Fullerene cages with 96 carbon atoms are required to generate Au_{50} antifullerene cages by dualization. There are 187 isomers of C_{96} provided in the fullerene structure library. All of these isomers were transformed into Au_{50} antifullerene cages by dualization. We therefore designate the isomers of Au_{50} antifullerene cages by the same number indices as their duals in the fullerene structure library.[31] DFT calculations were then performed to optimize the structural isomers of the Au_{50} cages. Similar to ref 20, we employed a DMol package[32] and adopted the generalized gradient approximation (GGA) with Perdew−Burke−Ernzerholf (PBE) functional[33] for exchange-correlation interaction. A DFT-based relativistic semi-core pseudopotential (DSPP) fitted to all-electron relativistic results,[34] and a double numerical basis set including d-polarization functions (DND) was used in the DFT calculations. The reliability of this PBE/DSPP/DND combination was validated in ref 20 by computations on small Au_n clusters ($n = 1-14$ and 20). Self-consistent field (SCF) calculations were carried out with a convergence criterion of 10^{-6} a.u. on the total energy and the electron density. Geometry optimizations with symmetry constraints were performed using a convergence criterion of 2×10^{-3} a.u. on maximum energy gradient and 2×10^{-3} Å on maximum displacement for each atom. To ensure high quality results, the real-space global orbital cutoff radius was chosen to be as high as 5.5 Å in the computations. Normal-mode analyses have been performed on the top 15 lowest-energy configurations to confirm that they are all true minima on the potential energy surface. For comparison, the lowest-energy cage and space-filling configurations for Au_{50} reported in ref 20 were also included in our calculations.

Among all of the Au_{50} antifullerene cages generated by dualization of C_{96} fullerenes, we find the No.185 cage with D_{6d} symmetry to have the lowest energy. Thus, the present lowest-energy D_{6d} cage is more favorable energetically by 0.255 and 0.411 eV than the C_2 cage and compact isomers, respectively, reported in ref 20. All three of these structures are depicted in Figure 1. In addition to the No.185 isomer with D_{6d} symmetry, several additional isomers were found having lower energies than the previously reported C_2 cage.[20] From lower to higher energy, these isomers are No. 180 (C_s), No. 115 (C_2), No. 182 (C_2), No. 178 (C_s), No. 118 (C_2), No. 146 (C_s), No. 114 (C_1), No. 155 (C_1), No. 130 (C_1), No. 175 (C_1), No. 144 (C_1), No. 164 (C_1), and No. 179 (C_2), respectively. Thus, there are at least 14 cage isomers having energies within ~0.25 eV that are more stable than the C_2 cage Au_{50} isomer from previous calculations.[20]

Figure 2 shows details of the structure of the new low energy D_{6d} isomer of Au_{50} with the different types of vertices color coded. Thus, consider the unique C_6 axis of this new D_{6d} Au_{50} antifullerene cage to be a polar axis with the north pole at one end and the south pole at the other end. The 50 gold atoms are then distributed as follows using geographical terminology:

polar degree 6 gold atoms (green): $2 \times 1 =$	2 atoms
circumpolar hexagons of degree 6 gold atoms (red): $2 \times 6 =$	12 atoms
temperate hexagons of degree 5 gold atoms (yellow): $2 \times 6 =$	12 atoms
tropical hexagons of degree 6 gold atoms (blue): $2 \times 6 =$	12 atoms
equatorial skew dodecagon of degree 6 gold atoms (orange): $1 \times 12 =$	12 atoms
Total number of gold atoms:	50 atoms

We now discuss the electronic properties of the lowest-energy Au_{50} antifullerene cage with D_{6d} symmetry. The HOMO−LUMO gap for the C_2 Au_{50} cage in ref 20 is 0.831 eV from both previous and current calculations, while the gap increases to 1.072 eV for the lowest-energy D_{6d} cage found in this work. Among all of the Au_{50} antifullerene cages studied (generated either by omnicapping or dualization of fullerene structures), the most stable D_{6d} cage has the largest HOMO−LUMO gap, in agreement with the previous observation in ref 20 that the HOMO−LUMO gap of the most stable Au_{50} isomer is the largest. Since the DFT-GGA calculations usually underestimate the electronic gap of molecules, the true gap of this D_{6d} cage is probably even larger. It is quite unusual to observe such large gap in a free-standing all-metal cluster with up to 50 atoms. On the contrary, the HOMO−LUMO gap for the compact

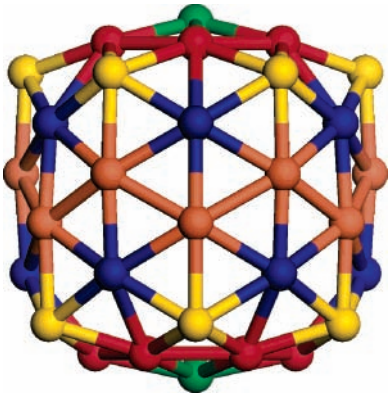

Figure 2. Details of the structure of the new low energy D_{6d} isomer of Au_{50} with the different types of vertices color coded.

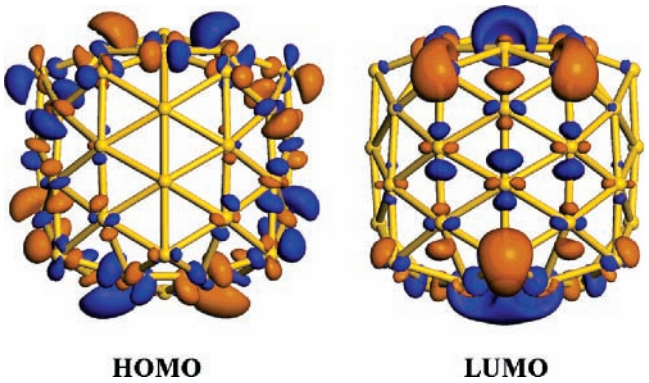

Figure 3. Isosurfaces for the electron wavefunction of the HOMO and LUMO of the No.185 antifullerene cage of Au_{50} with D_{6d} symmetry. Blue and gold colors denote different signs of the electron wavefunction.

structure shown in Figure 1 is only 0.23 eV.[20] It is noteworthy that the computed HOMO−LUMO gap for the Au_{32} cage (I_h) is 1.527 eV from the same PBE/DSPP/DND procedure.[20]

In Figure 3, we plot the isosurface for the electron wavefunction of the HOMO and LUMO of the D_{6d} cage of Au_{50}. First of all, both the HOMO and the LUMO are rather delocalized and distributed in the entire space of the cluster. However, careful examination shows that greater HOMO and LUMO electron densities are distributed on the two poles with less electron density in the equatorial region. The delocalized nature of electron density relates to the aromaticity of the cluster. It is interesting to ask why Au_{50} is so unique that a number of cage isomers have energies lower than or at least comparable to the space-filling structures. The unusual stability of Au_{32} and Au_{50} cages in previous work[19,20] were attributed to the effect of spherical aromaticity, and these two sizes fall into the $2(k+1)^2$ skeletal electron counting rule[22] for $k = 3$ and 4, respectively, by taking into account only the s valence electrons of Au. We have not computed the NICS value of the lowest energy D_{6d} cage of Au_{50} in this work. However, previous calculations in ref 20 suggest that the NICS values of the Au_{50} cages are not sensitive to the configuration and are around −80 ppm.

We have also examined the degeneracies of HOMO and LUMO for D_{6d} and C_2 cages presented in Figure 1. For the lowest-energy D_{6d} cage, both HOMO and LUMO are double degenerate, and there is another double degenerate molecular orbital lying only 0.013 eV lower than the HOMO. For the C_2 cage, there is no degeneracy for either HOMO or LUMO. According to group theory, the D_{6d} point group with a C6 axis has doubly degenerate irreducible representations, whereas the C_2 point group has only nondegenerate irreducible representation.

Population analysis of the lowest-energy Au_{50} cage (No. 185, D_{6d}) yields the average numbers of s, p, and d electrons as 1.06, 0.21, and 9.73, respectively. This indicates some electron transfer from the d orbitals to the s and p orbitals, particularly the p orbitals, relative to the original $s^1p^0d^{10}$ electronic configuration of an isolated Au atom. In previous work,[19] Gong and co-workers argued that relativistic effects result in strong s-d hybridization, which seems to account for the stability of the cage structures of Au clusters. In Figure 4, we plot the partial density of states of the Au_{50} cage. It is clear that there is simultaneous s, p, and d components for the electronic density of state at the Fermi level, similar to previous DFT calculations for the Au_{32} (I_h) cage.[19] It is noteworthy that the computed electron density of state should be basically independent of the choice of basis set. Indeed, we used plane-wave code (CASTEP) and observed a similar feature of the density of states.

The D_{6d} Au_{50} cage shown in Figure 1 can also be viewed as an embryo of a single-walled gold nanotube. Thus, if the north and south poles of the cage are removed, and the remaining section is used as a repeating unit cell to build a nanotube, a single-walled gold nanotube of 0.96 nm in diameter can be obtained. This gold nanotube can also be constructed from a (6,6) armchair carbon nanotube by dualization. In recent work, a hollow tube-like structure of a D_{6d} cage was proposed as the lowest-energy structure for Au_{26}, which can be also constructed

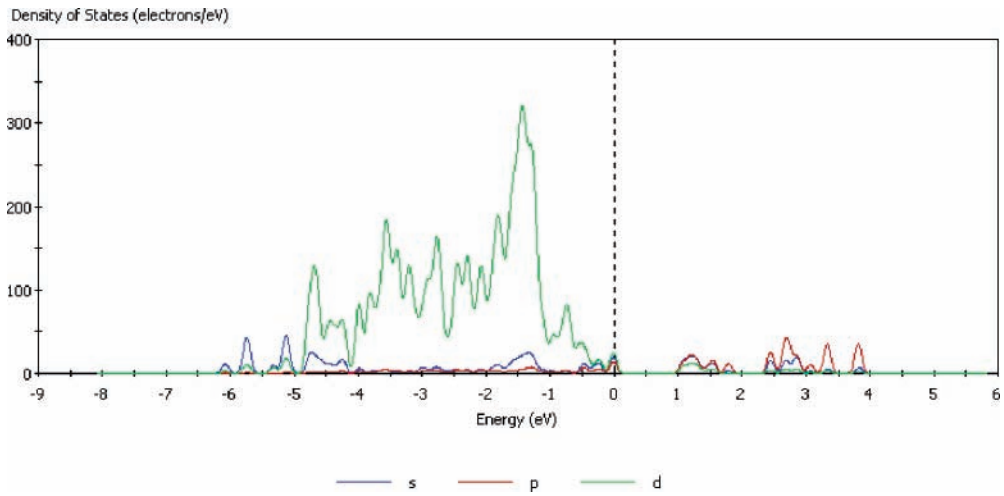

Figure 4. Partial density of states for s, p, and d components of the lowest-energy Au_{50} cage (D_{6d}). The position of the Fermi level indicated by the dashed line.

from a (6,0) zigzag single-walled carbon nanotube. The discovery of these embryonic tube-like structures in medium-sized gold clusters might be associated with the experimental observation of single-walled gold nanotubes.[25]

In summary, we have proposed two methods to construct gold antifullerene cages from carbon fullerene cages, namely omni-capping and dualization. In this connection, we have used dualization to generate 187 isomers of antifullerene cages of Au_{50}. Among these Au_{50} isomers, the lowest energy isomer is a D_{6d} cage, which is more stable than the previously proposed C_2 cage Au_{50} isomer by 0.255 eV. The unusual stability of these Au_{50} cages appears to arise from their spherical aromaticity and sp-d hybridization.

The discovery of highly stable gold antifullerene cages might lead to some potential applications. For example, they might be used to encapsulate guest atoms or molecules[36] or they could be incorporated inside the internal space of carbon nanotubes.[37] Either approach can provide opportunities for the electronic tuning of such hybrid structures.

Acknowledgment. The portion of the work in China was supported by the Young Teacher Foundation of Dalian University of Technology, Project No. 602003. The portion of the work in the U.S.A. was partially supported by the U.S. National Science Foundation Grant CHE-0209857.

References and Notes

(1) Haruta, M.; Kobayashi, T.; Sano, H.; Yamada, N. *Chem. Lett.* **1987**, *2*, 405.
(2) Bond, G. C.; Thompson, D. T. *Gold Bull.* **2000**, *33*, 41.
(3) Yoon, B.; Häkkinen, H.; Landman, U.; Wörz, A. S.; Antonietti, J. M.; Abbet, S.; Judai, K.; Ueli Heiz, U. *Science* **2005**, *307*, 403.
(4) Schwerdtfeger, P. *Angew. Chem., Int. Ed.* **2003**, *42*, 1892.
(5) Pyykko, P. *Angew. Chem., Int. Ed.* **2004**, *43*, 4412.
(6) Daniel, M. C.; Astruc, D. *Chem. Rev.* **2004**, *104*, 293.
(7) Wang, J. L.; Wang, G. H.; Zhao, J. J. *Phys. Rev. B* **2002**, *66*, 035418.
(8) Xiao, L.; Wang, L. C. *Chem. Phys. Lett.* **2004**, *392*, 452.
(9) Fernandez, E. M.; Soler, J. M.; Garzon, I. L.; Balbas, L. C. *Phys. Rev. B* **2004**, *70*, 165403.
(10) Olson, R. M.; Varganov, S.; Gordon, M. S.; Metiu, H.; Chretien, S.; Piecuch, P.; Kowalski, K.; Kucharski, S. A.; Musial, M. *J. Am. Chem. Soc.* **2005**, *127*, 1049.
(11) Furche, F.; Ahlrichs, R.; Weis, P.; Jacob, C.; Gilb, S.; Bierweiler, T.; Kappes, M. M. *J. Chem. Phys.* **2002**, *117*, 6982.
(12) Hakkinen, H.; Yoon, B.; Landman, U.; Li, X.; Zhai, H. J.; Wang, L. S. *J. Phys. Chem. A* **2003**, *107*, 6168.
(13) Gilb, S.; Weis, P.; Furche, F.; Ahlrichs, R.; Kappes, M. M. *J. Chem. Phys.* **2002**, *116*, 4094.
(14) Li, J.; Li, X.; Zhai, H. J.; Wang, L. S. *Science* **2003**, *299*, 864.
(15) Garzon, I. L.; Michaelian, K.; Beltran, M. R.; Posada-Amarillas, A.; Ordejon, P.; Artacho, E.; Sanchez-Portal, D.; Soler, J. M. *Phys. Rev. Lett.* **1998**, *81*, 1600.
(16) Michaelian, K.; Rendon, N.; Garzon, I. L. *Phys. Rev. B* **1999**, *60*, 2000.
(17) Li, T. X.; Yin, S. Y.; Ji, Y. L.; Wang, B. L.; Wang, G. H.; Zhao, J. J. *Phys. Lett. A* **2000**, *267*, 403.
(18) Johansson, M. P.; Sundholm, D.; Vaara, J. *Angew. Chem., Int. Ed.* **2004**, *43*, 2678.
(19) Gu, X.; Ji, M.; Wei, S. H.; Gong, X. G. *Phys. Rev. B* **2004**, *70*, 205401.
(20) Wang, J. L.; Jellinek, J.; Zhao, J. J.; Chen, Z. F.; King, R. B.; Schleyer, P. v. R. *J. Chem. Phys. A* **2005**, *109*, 9265.
(21) Gao, Y.; Zeng, X. C. *J. Am. Chem. Soc.* **2005**, *127*, 3698.
(22) Hirsch, A.; Chen, Z. F.; Jiao, H. *Angew. Chem., Int. Ed.* **2000**, *39*, 3915.
(23) Fa, W.; Dong, J. M. *J. Chem. Phys.* **2006**, *124*, 114310.
(24) Bulusu, S.; Li, X.; Wang, L. S.; Zeng, X. C. *Proc. Natl. Acad. Sci. U.S.A.* **2006**, *103*, 8326.
(25) Oshima, Y.; Onga, A.; Takayanagi, K. *Phys. Rev. Lett.* **2003**, *91*, 205503.
(26) Kroto, H. W.; Heath, J. R.; O'Brien, S. C.; Curl, R. F.; Smalley, R. E. *Nature* **1985**, *318*, 162.
(27) Sovov, S. C.; Corbet, J. D. *Science* **1993**, *252*, 880.
(28) Golberg, D.; Bando, Y.; Stephan, O.; Kurashima, K. *Appl. Phys. Lett.* **1998**, *73*, 2441.
(29) Bai, J.; Virovets, A. V.; Scheer, M. *Science* **2003**, *300*, 781.
(30) Zhao, J. J.; Xie, J. R. H.; Zhou, X. L.; Chen, X. S.; Lu, W. *Phys. Rev. B* **2006**, *74*, 035319.
(31) URL: http://www.cochem2.tutkie.tut.ac.jp/Fuller/fsl/fsl.html.
(32) DMOL is a density functional theory program distributed by Accelrys, Inc. Delley, B. *J. Chem. Phys.* **1990**, *92*, 508; *J. Chem. Phys.* **2000**, *113*, 7756.
(33) Perdew, J. P.; Burke, K.; Ernzerhof, M. *Phys. Rev. Lett.* **1996**, *77*, 3865.
(34) Delley, B. *Phys. Rev. B* **2002**, *66*, 155125.
(35) Schleyer, P. v. R.; Maerker, C.; Dransfeld, A.; Jiao, H.; Hommes, N. J. R. v. E. *J. Am. Chem. Soc.* **1996**, *118*, 6317.
(36) Gao, Y.; Bulusu, S.; Zeng, X. C. *J. Am. Chem. Soc.* **2005**, *127*, 15680.
(37) Zhao, J. J.; Wen, B.; Zhou, Z.; Chen, Z. F.; Schleyer, P. v. R. *J. Comput. Theor. Nanosci.* **2006**, *3*, 459.